16th World Conference on Earthquake, 16WCEE 2017
Santiago Chile, January 9th to 13th 2017
Paper N°4908
Registration Code: S-A1462984296

CYCLIC BEHAVIOR OF PRECAST HIGH-STRENGTH REINFORCED CONCRETE

Yu-Chen Ou [(1)], H. Alrasyid[(2)], Z.B. Haber[(3)],Hung-Jen Lee [(4)]
[(1)] *Professor, National Taiwan University of Science And Technology, yuchenou@mail.ntust.edu.tw*
[(2)] *Assistant Professor, Institut Teknologi Sepuluh Nopember, harun@ce.its.ac.id*
[(3)] *Engineer, Genex Systems, zacharyhaber@hotmail.com*
[(4)] *Associate Professor, National Yunlin University of Science and Technology, leehj@yuntech.edu.tw*

Abstract

Double-curvature cyclic tests of large-scale columns were conducted to investigate the seismic performance of precast high-strength reinforced concrete columns. High-strength concrete and high-strength longitudinal and transverse reinforcement were used. The use of grouted coupler splices for the high-strength longitudinal reinforcement in the plastic hinge zone and the use of butt-welded splices for the high-strength transverse reinforcement were examined. Test results showed that precast columns with the grouted coupler splices exhibited comparable seismic performance with monolithic counterparts. The butt-welded splice had a negligible effect on the tensile behavior of the spliced bars. However, precast columns with such welded splices in transverse reinforcement showed smaller ultimate drift capacities than their counterparts with hooked transverse reinforcement. This was due to the reduced resistance of butt-welded transverse reinforcement to buckling of longitudinal reinforcement..

Keywords: high-strength concrete; high-strength reinforcement; grouted coupler splice; butt-welded splice

1. Introduction

Reinforced concrete (RC) structures have the advantages of lower cost, higher stiffness, and better sound insulation than steel structures. However, when used in high-rise buildings, traditional cast-in-place RC structures are usually less attractive than steel structures due to two major issues: large column sizes in lower stories and low construction speed. The former issue can be addressed by using high-strength materials and the latter by using precast construction. This study investigates the seismic behavior of precast high-strength RC columns and is a part of Taiwan New RC research effort which aims to develop high-strength RC structures for high-rise building construction.

This study used high-strength longitudinal (SD685) and transverse (SD785) steel reinforcement having specified yield strengths of f_{yls} = 685 MPa (100 ksi) and f_{yts} = 785MPa (114 ksi), respectively. High-strength concrete with a specified compressive strength of f'_{cs} = 70 MPa (10 ksi) was also used. The SD685 longitudinal reinforcement and SD785 transverse reinforcement were originally developed in Japan[1] and slightly modified by Taiwan Concrete Institute (TCI)[2]. The specifications of the two types of reinforcement can be found in Ou and Kurniawan[3]. Hwang et al[4] examined the cyclic behavior of five large-scale columns under axial load ratios of 0.42-0.67 ($P/A_g f'_c$) with concrete f'_c of 83-112 MPa (12-16 ksi), and with the SD685 and SD785 reinforcement. A confinement design equation modified from the CSA A23.3-04[5] confinement equation was proposed for such high-strength columns. Test results showed that the proposed equation can be conservatively used to design confinement reinforcement to achieve a drift capacity of $\geq$ 3%. Ou and Kurniawan[3],[6] investigated the shear behavior of 16 shear-critical large-scale columns with f'_c of 93-139 MPa (14-20 ksi) and with the SD685 and SD785 reinforcement. Test results showed no yielding in the SD785 transverse reinforcement at peak applied load. This observation is consistent with the findings of earlier studies on high-strength columns[7],[8].

Prefabricated butt-welded hoops were used in this study. The use of welded splices eliminates the possibility of pullout failure of hook anchorages and reduces reinforcement congestion. However, the ACI 318 code[9] does not permit longitudinal or transverse reinforcement to employ welded splices in plastic hinge zones. This is because the ACI 318 code only requires welded splices resisting earthquake-induced forces to develop 1.25 f_{ys} of the spliced bars, same as for type 1 mechanical splices, and reinforcement stress in plastic hinge zones can exceed 1.25 f_{yt}. Restrepo et al[15] tested bridge columns with butt-welded hoops and showed that butt-welded hoops can be used for A706 reinforcement16. However, butt-welded hoops should not be used for the high-strength reinforcement examined (f_{yt} =827 MPa or 120 ksi) in the plastic hinge zones due to the limited strain capacity at peak tensile force of the welded hoops. The welded splices used in this study were able to develop the specified tensile strength of the spliced bars, same as for type 2 mechanical splices. They were used in the entire column including the plastic hinge zone.

This study tested six large-scale columns to examine the seismic behavior of precast high-strength RC columns. The effect of using grouted coupler splices for longitudinal reinforcement and butt-welded splices for transverse reinforcement in the plastic hinge zone was evaluated by comparison with monolithic columns with conventional details. One unique aspect of this project is that the high-strength columns tested had 600×600 mm (23.62 × 23.62 in) square cross-sections. Thus they are considerably larger-scale than those tested in previous studies [1],[7],[8],[14],[17].

2. Experimental Program

2.1. Column design

Six large-scale high-strength columns were tested. Table 1 lists the column design parameters and Fig. 1 illustrates the reinforcement and cross-sectional details of each column. The nomenclature of the columns is as follows: "C" and "G" denote conventional monolithic column and precast column with grouted splice, respectively; "H" and "W" denote transverse reinforcement with hook anchorage and welded splice, respectively; and "10" and "33" denote axial load of 0.1 and 0.33 $A_g f_c^{'}$, respectively. A set of three columns were tested under low axial load (0.1 $A_g f_c^{'}$), and a second set of three were tested under high axial load (0.33 $A_g f_c^{'}$). In each group of three, one baseline column was designed using transverse hoop reinforcement with seismic hook anchorages and was monolithically constructed (CH10 and CH33). The remaining two columns in each group (four columns total) were precast and employed grouted couplers within the lower plastic hinge zone for the column-footing joint. Two precast columns used transverse hoop reinforcement with seismic hook anchorages (GH10 and GH33), and two used butt-welded splices (GW10 and GW33). The monolithic columns (CH10 and CH33) served as baselines to evaluate the effect of grouted couplers on column performance, and the effect of transverse reinforcement anchorage was evaluated using the precast models. Lastly, effect of axial load could be examined by the comparing the two groups of three.

Table 1 – Column design parameter

Name	Concrete	Longitudinal Reinforcement SD685					Transverse Reinforcement SD785						Axial load
	$f_c^{'}$ (MPa)	Size	ρ_g (%)	Splice	f_{yl} (MPa)	f_{ul} (MPa)	Size	s (mm)	ρ_s (%)	Type	f_{yt} (MPa)	f_{ut} (MPa)	$\frac{P}{A_g f_c^{'}}$
CH10	77	16 D25	2.18	C	713	932	D13	100	2.12	H	886	1095	0.1
GH10	74			G			D13		2.12	H	886	1095	0.1
GW10	73			G			D13		2.12	W	868	1104	0.1
CH33	75			C			D16		3.20	H	836	1020	0.33
GH33	77			G			D16		3.20	H	836	1020	0.33
GW33	77			G			D16		3.20	W	818	1022	0.33

$f_c^{'}$ =compressive strength of concrete; ρ_g =ratio of area of longitudinal reinforcement to gross area of column section; f_{yl} =yield strength of longitudinal reinforcement; f_{ul} =ultimate strength of longitudinal reinforcement; ρ_s =ratio of volume of transvers reinforcement to gross area of column section; f_{yt} =yield strength of transverse reinforcement; f_{ut} =ultimate strength of transverse reinforcement; C : continue without splice; G=grouted coupler splice; H=hooked anchorage W=welded splice

All the columns were designed with high-strength SD685 longitudinal steel reinforcement, SD785 transverse steel reinforcement, and concrete having a specified compressive strength of 70 MPa (10 ksi). Measured material properties are listed in Table 1 along with other column design details. Each measured property was obtained from the average of three samples. Columns tested under 0.1 and 0.33 $A_g f_c^{'}$ were designed to have flexural strengths of 1686 and 1919 kN-m (1243 and 1415 kips-ft), respectively. The longitudinal reinforcement ratio was 2.18% for all columns, which is representative of many building columns. The volumetric ratios of transverse reinforcement for low and high axial load columns were 2.12% and 3.20%, respectively and were determined based on the confinement equation proposed by Hwang et al[4].

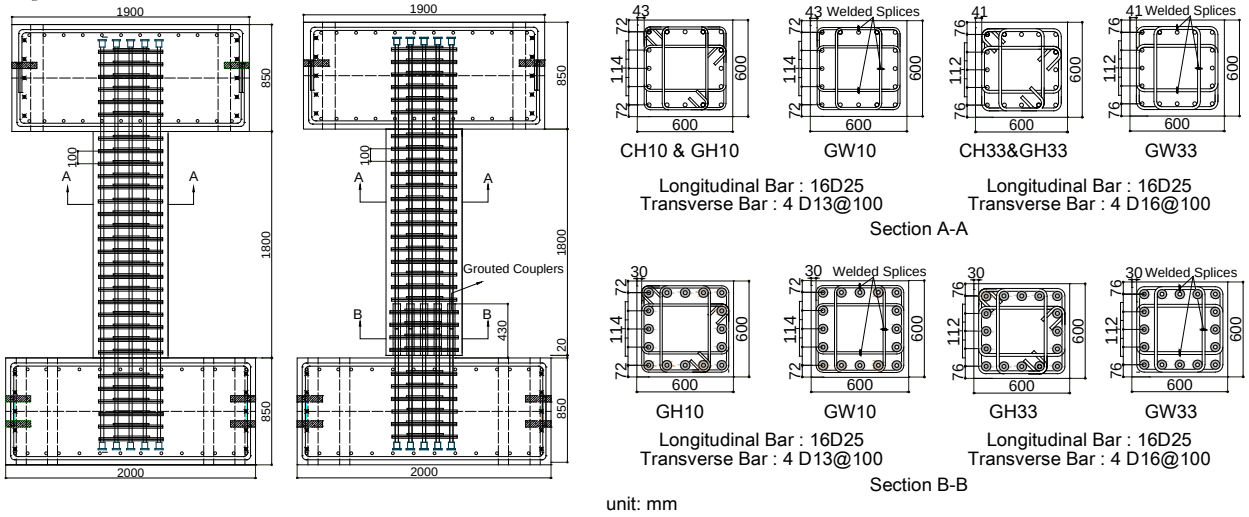

(a) (b) (c)

Fig. 1 – Cross Sectional Details (a)columns without grouted couplers (b) column with grouted couplers (c) section design

2.2. Splice Testing

Uniaxial load tests were conducted on the grouted splice assembly to quantify the behavior of these splices according to the TCI acceptance criteria[22]. Tests were conducted using the same grouted couplers and longitudinal bars (D25 – SD685) as those used for precast column construction. During loading, specimens were subjected to load reversals to determine if permanent deformation occurred within the assembly, otherwise referred to as "slip". A summary of test results exhibited that in both monotonic and cyclic tests, specimens were able to develop the 1.25 times the specified yield strength (ACI 318, Type 1 requirement) and the specified tensile strength (ACI 318, Type 2 requirement) of the spliced bars. The grouted couplers also satisfied the SA criteria, which is the highest performance level specified by TCI [22] In all cases, splices failed by pullout of the reinforcing bar from the grouted coupler. Prior to failure, the maximum strain developed in the bars at ultimate splice bar assembly ranged from 0.049 to 0.079, which should be adequate to withstand the strain demands in building columns.

A series of butt-welded splices were tested under monotonic tensile loading until failure. Three samples for each bar size with the butt weld located in the middle of the samples were tested. Test results showed fracture occurred in the bar away from the weld. The average elongation was 11% and 13% for D13 and D16 bar splices, respectively. The elongations are similar to those obtained from tensile testing of bars only, which were 12% and 13%, respectively, which indicates that butt-welded splices had a negligible effect on the mechanical behavior of the bars.

2.3. Construction of columns

Columns CH10 and CH33 were constructed as would conventional building columns and were cast monolithically. The precast columns (GH10, GW10, GH33, and GW33) were constructed in two pieces. The upper piece included the upper footing, the column, and the grouted coupler sleeves as shown in Fig. 2a. Figure 2b depicts the high-strength butt-welded hoops that were used in constructing the column of GW10 and GW33. The lower footing was constructed second and included longitudinal reinforcing bar dowels for the grouted coupler connection (Fig. 2c). The two pieces were joined together by placing the upper piece on the top of the lower piece with protruding bars being inserted into the coupler holes at the bottom of the column. A 20-mm (0.79-in) bedding layer was formed between the lower and upper pieces using steel shims (Fig 2c). High-strength cementitious grout with a compressive strength of 120 MPa (17.4 ksi) was pumped into the bedding layer and

through the couplers using inlet ports at the bottom of the column until it flowed from the outlet ports at the top of the couplers (Fig. 2d). The ports were plugged and assembly process was completed.

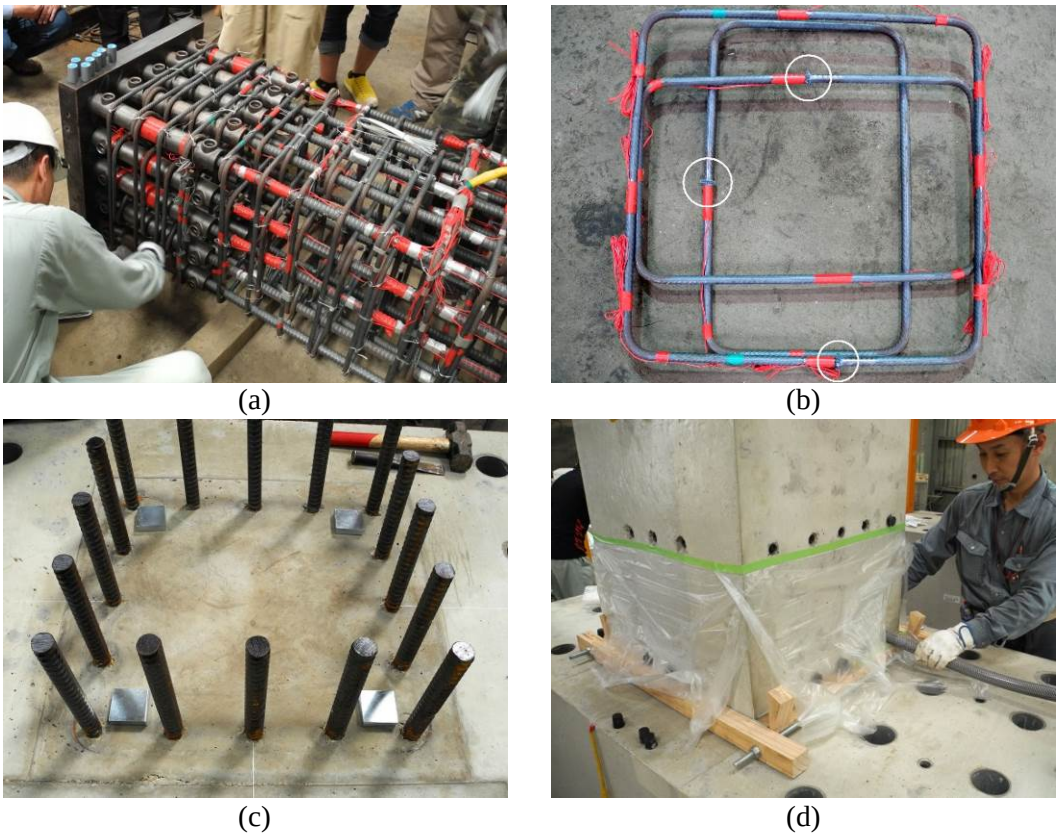

(a) (b)

(c) (d)

Fig. 2 – (a) Grouted coupler splices at the column base; (b) welded spliced hoops (welded locations indicated by circles); (c) top face of the lower piece with steel shims for bedding layer and longitudinal reinforcing bar dowels; and (d) grouting operation

2.4. Test Setup and Instrumental

The columns were tested using displacement-controlled double-curvature cyclic loading under constant axial load. The cyclic loading was based on ACI 374.1-05[26] and contained nominal drift ratios of 0.25%, 0.375%, 0.5%, 0.75%, 1%, 1.5%, 2%, 3%, 4%, 5%, 6%, and 7%. The actual drift ratio achieved for each drift level was smaller than the nominal value. Three full cycles were applied at each drift ratio. An optical motion tracking system was used to monitor the coordinates of twenty sensors installed on the column and the footings to capture column deformations during testing. Strain gauges were installed on longitudinal reinforcement, transverse reinforcement and grouted couplers to monitor strain response at various locations during testing.

3. Test Result and Discussion

3.1. Force-displacement relationship and damage

The lateral force versus drift relationship for each column is shown in Fig. 6, in which the $P-\Delta$ effect due to the lateral movements of applied axial load has been removed. Important events are indicated in the figure: idealized yield point, peak applied load, yielding of longitudinal or transverse reinforcement, buckling of longitudinal reinforcement, and fracture or anchorage failure of transverse reinforcement. Force-displacement

relationships were idealized using a bilinear relationship which was determined according to the procedures outlined in FEMA 356[27]. The ultimate point is the point in the actual envelope response after the peak applied load that has a force equal to 80% of the peak applied load. The idealized yield drift, peak applied load, ultimate drift and ductility were averaged from positive and negative drift cycles and are listed in Table 3.

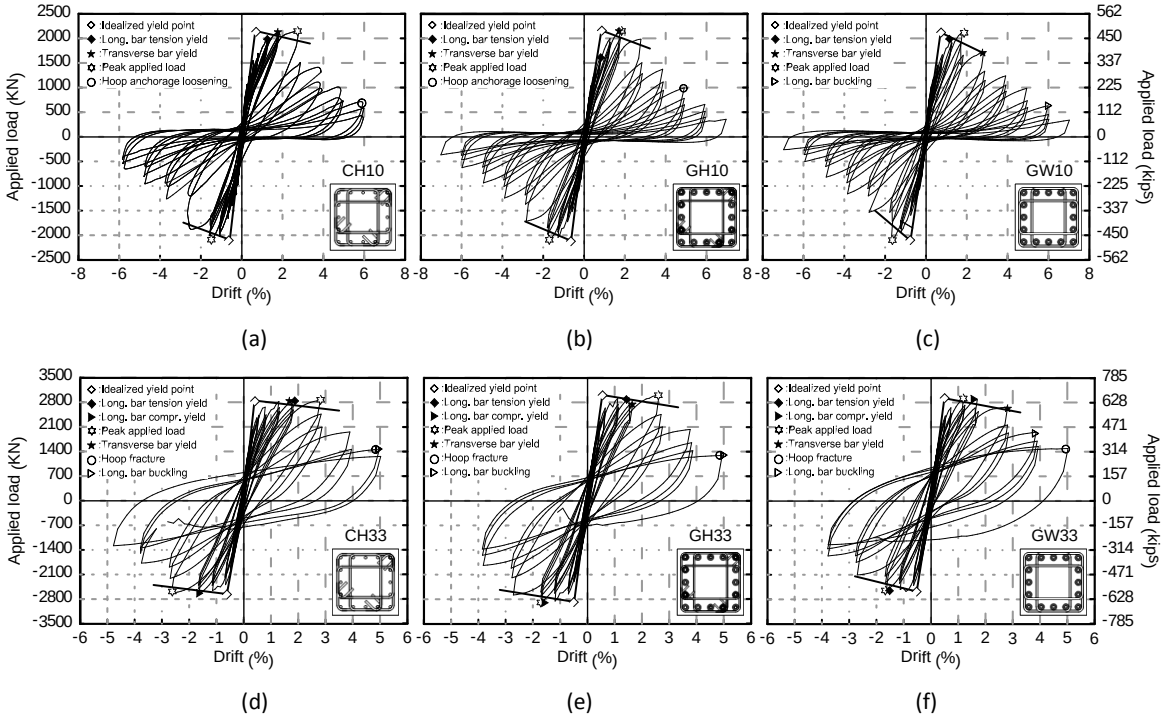

Fig. 3 – Hysteretic behavior (a) CH10; (b)GH10; (c)GW10; (d)CH33; (e) GH33; (f)GW 33

Table 2 – Forces and displacements capacities

Name	Idealized Yield Drift (%)	Peak Load (kN)	Ultimate Drift (%)	Ductility
CH10	0.62	2121	3.10	5.0
GH10	0.74	2136	3.06	4.1
GW10	0.77	2115	2.68	3.5
CH33	0.51	2752	3.40	6.7
GH33	0.52	2942	3.27	6.3
GW33	0.51	2749	3.03	6.0

For low axial load columns, the first flexural crack, flexural-shear crack, and web-shear crack occurred at nominal drift ratios of 0.375%, 0.5%, and 0.75%, respectively. This cracking pattern can still be observed at 1.5% nominal drift along with initiation of cover concrete spalling at the toe and heel of each column (Figs. 4a-c). Starting from 2% nominal drift, the column with welded hoops (GW10) began to exhibit wider cracks between cover and core concrete compared with CH10 and GH10. This can be observed in Figs. 4(g)-(i) which compares the cracking patterns of these columns at 3% nominal drift. The wider cracks in GW10 were caused by larger average laterally unsupported length of longitudinal reinforcement compared with that of CH10 and GH10. The elimination of hook anchorage reduces the number of hoop bars providing lateral support from two to one at the locations of hook anchorage consequentially increasing the average laterally unsupported length. This accelerated buckling of longitudinal reinforcement and resulted in earlier spalling of cover concrete and quicker post-peak lateral load degradation. This also resulted in reduced ultimate drift and ductility. Compared with GH10, the ultimate drift and ductility of GW10 were reduced by 12% and 15%, respectively (Table 3).

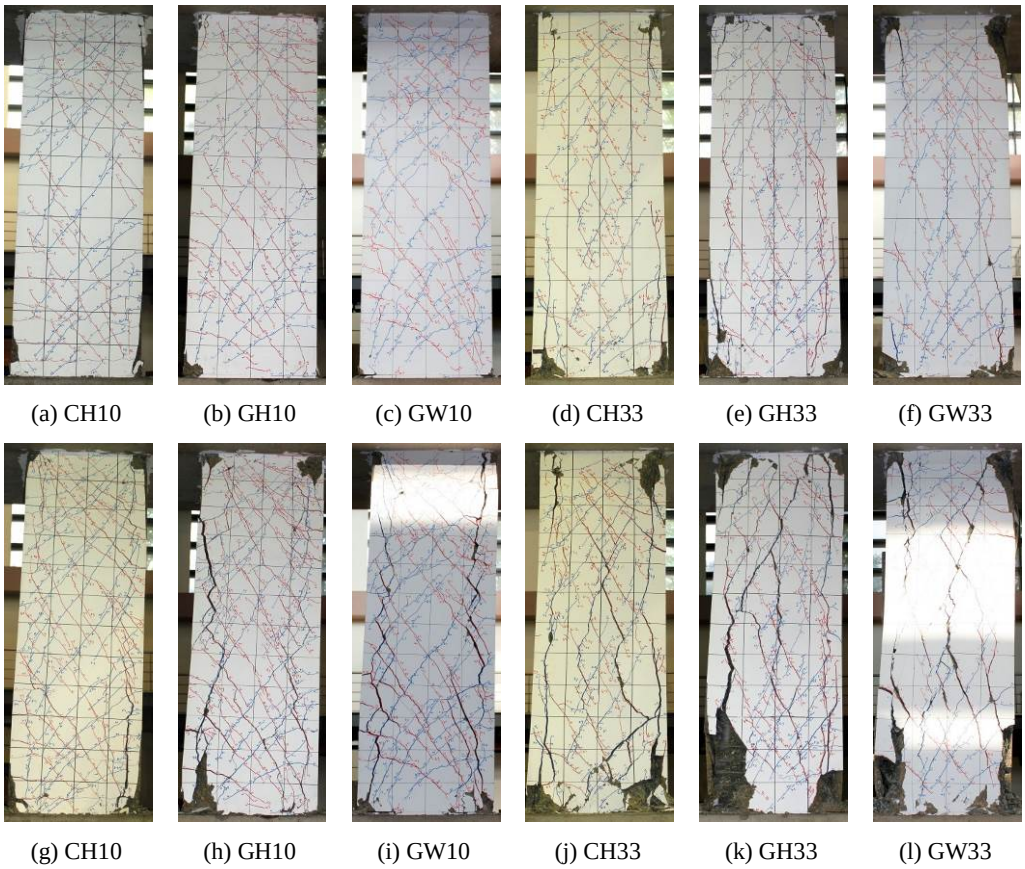

(a) CH10 (b) GH10 (c) GW10 (d) CH33 (e) GH33 (f) GW33

(g) CH10 (h) GH10 (i) GW10 (j) CH33 (k) GH33 (l) GW33

Fig. 4 – Damage conditions at 1.5% nominal drift (a-f) and 3% nominal drift (g-i)

For columns under high axial load, the first flexural, flexural-shear, and web-shear cracks occurred at 0.375%, 0.5%, and 0.5% nominal drifts, respectively. Web-shear cracks appeared earlier than those in low axial load columns because of higher shear demand due to increased axial load. Moreover, increased axial load resulted in steeper web-shear cracks than those in low axial load columns which can be observed by comparing Figs. 4d-f to 4a-c. At 1.5% nominal drift, comparable crack patterns and spalling of cover concrete was observed among the columns with high axial load (Fig. 4d-f). The peak applied loads of high axial load columns were reached at nominal drifts of 2-3%. Visible widening of web-shear cracks and vertical cracks between core and cover concrete started at 2% nominal drift. As drift levels increased, cracks continued to widen and number of wide cracks increased (Fig. 4j-l). Compared with CH33 and GH33, GW33 showed faster strength degradation after reaching the peak applied load due to increased laterally unsupported length as discussed previously in low axial load columns. Compared with GH33, GW33 showed 7% and 5% reduction in the ultimate drift and ductility, respectively. At 4% nominal drift, the longitudinal reinforcement in the column with welded hoops (GW33) showed visible buckling. The longitudinal reinforcement in the other two columns (CH33 and GH33) did not show visible buckling until the following drift level (5% nominal drift). This observation supported the statement above that relates the faster strength degradation of GW33 to the earlier buckling of longitudinal reinforcement. Soon after the visible buckling of longitudinal reinforcement the transverse reinforcement of the three columns fractured at 5% nominal drift due to extensive kinking and localized plastic straining. The columns suddenly lost their axial load carrying capacity and the tests could not be continued. Based on bilinear idealization, the three columns under high axial load showed a similar idealized yield drift. The decrease effect in initial stiffness of gaps resulting from precast construction was minimized due to high axial load. The monolithic column (CH33) showed the highest ductility than the other two columns (Table 3).

3.2. Transverse reinforcement strain

The measured strain responses in transverse reinforcement showed that the maximum strain exceeded the yield strain in all columns prior to reaching ultimate drift capacity. No clear trend of difference in strain responses was observed between monolithic and precast columns, and between hoops with hook anchorage and welded hoops. The detailing requirement of the current ACI 318 code for hook anchorage was adequate for SD785 transverse reinforcement.

The low and high axial load columns started to show significant softening in hysteretic behavior at 2% and 1.5% nominal drifts, respectively. After which point, wide cracks were observed as previously mentioned and dilation of confined core concrete, otherwise referred to as the "confinement effect," started to play a significant role in increasing the strain in transverse reinforcement. Prior to these drift levels, shear deformation was the main contributor to strain in the transverse reinforcement. The maximum strains developed in transverse reinforcement at these drift levels were approximately 0.0035-0.004 and 0.002 for low and high axial load columns, respectively. The 0.0035-0.004 and 0.002 strains provided evidence that shear was able to develop a stress in transverse reinforcement as high as 700-800 MPa (100-116 ksi) and 400 MPa (58 ksi) in low and high axial load columns, respectively. Note that since the columns did not fail in shear at the two drifts, the observed maximum strains may be higher if shear continued to increase and hence cannot be used to set the upper limit on transverse reinforcement stress for shear design.

3.3. Shear deformation, curvature and strain of longitudinal reinforcement

Using an optical motion tracking system the column deformations were monitored. The measured deformations at 2% and 0.75% nominal drift for low and high axial load columns, respectively, were decomposed into shear strains and curvatures along the length of each column. Shear strain was spread uniformly along the height of each column. Thus, it can be inferred that the test variables had little influence on the shear deformation of these columns. As would be expected, the largest curvatures were measured at the column joint locations of each where the maximum moments occur. Curvatures measured at the bottom of the column were larger for the precast columns (GH10, GW10, GH33, and GW33) than for monolithic columns (CH10 and GH10). This behavior was caused by the presence of grouted couplers which stiffen the connection region and result in reduced rotation capacity of the plastic hinge. Reduced rotation capacity requires redistribution of elastic and plastic deformations within the column to achieve the lateral displacement demand. Whereas the rotation demand of the monolithic columns is distributed throughout the plastic hinge zone, it was shown by Haber et al.10 that the rotation demand of the precast columns primarily occurs at the joint between the column and the adjacent member. This was further substantiated by examining the distribution of flexural cracks in columns with grouted coupler compared to monolithic columns (Fig. 4a-f). No flexural cracks were observed in the bottom 150-mm (6-in) region (from the column base to the first horizontal grid line) in precast columns while at least one was observed in monolithic columns. A slight increase in curvature from the region covering the top end of the grouted couplers was observed for one of the precast columns in low axial load (GH10).

Based on the measured deformations, the lateral displacement of the columns was decomposed in percentage contribution from shear deformation, flexural deformation and concentrated rotation due to bar slip at the joints. Shear contribution was in average 30% at 2% nominal drift for low axial load columns. For high axial load columns, shear contribution increased significantly to approximately 50% when significant cracking started to occur at 1.5% nominal drift for GH33 and 1.0% nominal drift for GW33. The high contribution of shear to the column displacement was due to the low a/h of 1.5, which is common for lower story columns in high-rise buildings.

The measured maximum tensile strains in longitudinal reinforcement at the base of the low axial load columns were 0.0093, 0.013, and 0.0072 for CH10, GH10, and GW10. For high axial load columns, these strains were 0.0082, 0.0034, and 0.0039 for CH33, GH33, and GW33. These strains were much smaller than the maximum strain measured in the bar-splice assembly tests. This confirms that the grouted couplers examined can be used in the plastic hinge zones of the columns tested. The strains directly above the grouted coupler, 455 mm (18 in)

above the base, were approximately the yield strain (Figs. 12b and 12d). Moment-curvature analysis shows that the tensile strain at this location is much lower than the yield strain. The increase in the actual strain was due to the tension shift effect caused by flexural-shear cracks around the top of grouted couplers (Fig. 4). In other words, the tension shift effect increased the demand to the upper portion of the coupler.

4. Conclusion

This study investigated the seismic performance of large-scale precast high-strength RC columns tested using double-curvature cyclic loading. The use of grouted coupler splices for the SD685 longitudinal reinforcement in the plastic hinge zone and butt-welded splices for the SD785 transverse reinforcement were examined. Important conclusions are summarized as follows:

(1) The bar-splice assembly testing showed that the grouted coupler splice was capable of developing the specified tensile strength of SD685 reinforcement. Although bar-splice assemblies failed by bar pull-out, the maximum strains measured in the spliced bars before failure were 0.049-0.079, which should be sufficient based on column test results. Column tests indicated that maximum tensile strain in the spliced bars close to the grouted couplers were 0.013 and 0.0034 under low and high axial load, respectively, which were well below the measured capacity of the splice. The precast columns with such splices and with hooked transverse reinforcement (GH10 and GH33) showed comparable seismic performance with monolithic counterparts (CH10 and CH33).

(2) Testing of bar-splice assemblies showed that the butt-welded splice had a negligible effect on the tensile behavior of the spliced bars. The assemblies fractured in the bars away from the weld location. However, testing of columns showed that the columns with such splices in the transverse reinforcement (GW10 and GW33) showed a faster post-peak strength degradation, which resulted in smaller ultimate drifts than their counterparts with hooked transverse reinforcement (GH10 and GH33). This was due to increased average laterally unsupported length and hence earlier buckling of longitudinal reinforcement in columns with welded transverse reinforcement compared with hooked transverse reinforcement.

5. Acknowledgement

Experimental study of this research was supported by Tokyo Tekko Co Ltd., Japan and conducted at National Center for Research on Earthquake Engineering (NCREE), Taiwan. Support for a visiting research assistant position at NCREE to the third author was provided by the National Science Foundation (US) East Asia and Pacific Summer Institutes (EAPSI) program and Ministry of Science and Technology (Taiwan).

6. Reference

[1] Aoyama, H., "Design of Modern Highrise Reinforced Concrete Structures." Imperial College Press, London, UK, 2001, 391 pp.
[2] TCI New High-Strength Reinforced Concrete Committee, "Steel bars for concrete reinforcement – SD550W, SD685, SD785," Taiwan Concrete Institute (TCI), Taipei, Taiwan, 2014, 10 pp.
[3] Ou, Y.C., Kurniawan, D.P., "Shear Behavior of Reinforced Concrete Columns with High-Strength Steel and Concrete," *ACI Structural Journal*, V. 112, No. 1, Jan.-Feb. 2015, pp. 35-45.
[4] Hwang, S.J., Hwang, G.J., Chang, F.C., Chen, Y.C., Lin, K.C., "Design of Seismic Confinement of Reinforced Concrete Columns Using High-Strength Materials," *Reinforced Concrete Columns with High Strength Concrete and Steel Reinforcement*, SP-293, American Concrete Institute, Farmington Hills, Mich., 2013, pp. 21-34.
[5] CSA Committee A23.3, "Design of Concrete Structures (CSA A23.3-04)," Canadian Standard Association, Mississauga, Canada, 2004, 214 pp.
[6] Ou, Y.C., Kurniawan, D.P., " Effect of Axial Compression on Shear Behavior of High-Strength Reinforced Concrete Columns," *ACI Structural Journal*, V. 112, No. 2, Mar.-Apr. 2015, pp. 209-219.

[7] Watanabe, F., Kabeyasawa, T., "Shear Strength of RC Members with High-Strength Concrete," in *High-Strength Concrete in Seismic Regions*, SP-176, American Concrete Institute, Farmington Hills, Mich., 1998, pp. 379-396.
[8] Maruta, M., "Shear Capacity of Reinforced Concrete Column Using High Strength Concrete," *The Eighth International Symposium on Utilization of High-Strength and High-Performance Concrete*, Tokyo, Japan, Oct. 27-29, 2008.
[9] ACI Committee 318, "Building Code Requirements for Structural Concrete (ACI 318-11) and Commentary ", American Concrete Institute, Farmington Hills, Mich., 2011, 503 pp.
[10] Haber, Z.B., Saiidi, M.S., Sanders, D.H.,"Seismic Performance of Precast Columns with Mechanically Spliced Column-Footing Connections," *ACI Structural Journal*, V. 111, No. 3, May-June, 2014, pp. 639-650.
[11] Ameli, M.J., Parks ,J.E., Brown,D.N., Pantelides,C. P., Sletten, J., and Swanwick, C., "Seismic Evaluation of Grouted Splice Sleeve Connections for Precast Reinforced Concrete," *The Seventh National Seismic Conference on Bridges & Highways*, Calif. , 20-22 May. 2013.
[12] Aida, H., Tanimura, Y., Tadokoro, T., and Takimoto, K., "Cyclic Loading Experiment of Precast Columns of Railway Rigid-Frame Viaduct Installed with NMB Splice Sleeves," *Proceedings of the Japan Concrete Institute*, V. 27, No. 2, 2005, pp. 613-618.
[13] Huang, S.W., Yu, J. T, Chiou, H.D., Asakawa, T. and Tsai, K.C.,, "Final Report of Experiment on Precast Reinforced Concrete Beam-Column Assemblage," *Report*, Chinese Society of Structural Engineering, 1997, 119 pp.
[14] Matsumoto T., Nishihara H., Nakao M., "Flexural Performance on RC and Precast Concrete Columns With Ultra High Strength Materials Under Varying Axial Load," *14th World Conference on Earthquake Engineering*,Beijing,China, Oct. 12-17, 2008.
[15] Restrepo, J.I., Seible, F., Stephan, B., Schoettler, M.J., "Seismic testing of bridge columns incorporating high-performance materials," *ACI Structural Journal*, V. 103, No. 4, July-Aug., 2006, pp. 496-504.
[16] ASTM A706/A706M-09b, "Standard Specification for Low-Alloy Deformed and Plain Bars for Concrete Reinforcement," ASTM International, West Conshohocken, Pa., 2009, 6 pp.
[17] Sakaguchi, N., Yamanobe, K., Kitada, Y., Kawachi, T. and Koda, S., "Shear Strength of High-Strength Concrete Members", *Second International Symposium on High-Strength Concrete*, SP-121, American Concrete Institute, Farmington Hills, Mich., 1990, pp. 155-178.
[18] NZS Committee P 3101," Concrete structures standard - The design of concrete structures (NZS3101 Part 1) ", Standards New Zealand,Wellington, New Zealand, 2006, 256 pp.
[19] ACI Innovation Task Group 4, "Report on Structural Design and Detailing for High-Strength Concrete in Moderate to High Seismic Applications (ITG-4.3R-07)," American Concrete Institute, Farmington Hill, Mich., 2007, 66 pp.
[20] ACI Committee 318, "Building Code Requirements for Structural Concrete (ACI 318-14) and Commentary (ACI 318-14R) ", American Concrete Institute, Farmington Hills, Mich., 2014, 524 pp.
[21] Elwood, K.J., Maffei, J., Riederer, K.A., Telleen, K., "Improving Column Confinement Part 2: Proposed new provisions for the ACI 318 Building Code," *Concrete International*. V. 31, No. 12, Dec. 2009, pp. 41-48.
[22] TCI New High-Strength Reinforced Concrete Committee, " Guidelines for Performance Evaluation of Mechanical Splices for High-Strength Steel Reinforcing Bars (Draft)," Taiwan Concrete Institute (TCI), Taipei, Taiwan, 2014.
[23] AC133, "Acceptance Criteria for Mechanical Connector Systems for Steel Reinforcing Bars." International Code Council Evaluation Service, 2010, 7 pp.
[24] Rowell, S. P., Grey, C. E., Woodson, S. C., and Hager, K. P., "High Strain-Rate Testing of Mechanical Couplers," *Report* ERDC TR-09-8, US Army Corps of Engineers, Sept. 2009.
[25] Haber, Z.B., Saiidi, M.S., and Sanders, D.H., "Precast Column-Footing Connections for Accelerated Bridge Construction in Seismic Zones," *Report* No. CA13-2920, Center for Civil Engineering Earthquake Research, Department of Civil and Environmental Engineering, University of Nevada, Reno, Nev., May 2013. 502 pp.
[26] ACI commite 374, "Acceptance Criteria for Moment Frames Based on Structural Testing and commentary (ACI 374.1-05)," American Concrete Institute, Farmington Hills, Mich., 2005, 9 pp.
[27] FEMA 356, "Prestandard And Commentary For The Seismic Rehabiltiation of Buildings," Federal Emergency Management Agency, D.C., 2000, 518 pp.